Molecular Dynamics Study of the Solid-State Structures of Linear-Low-Density Polyethylenes with Blocky Branches

Chunli Li and Phillip Choi*

Department of Chemical and Materials Engineering, Edmonton, Alberta, Canada T6G 2G6

Received May 16, 2008; Revised Manuscript Received July 29, 2008

ABSTRACT: Solid-state structures formed in the early stage of crystallization of linear-low-density polyethylene models (branch content = 10 hexyl branches per 1000 backbone carbons) with all branches clustered near chain ends (end type) and chain middles (middle type) were studied using molecular dynamics (MD) simulation. Crystallization of a 50/50 mol/mol blend of the aforementioned two types of branched chains and of such chains with linear chains, also 50/50 mol/mol, was also studied. The MD results showed that the end type chains tended to exhibit a slightly higher degree of order upon crystallization, as quantified by a higher *trans*/*gauche* (*t*/*g*) ratio than the middle type chains. This seems to relate to the fact that the end type chains had longer crystallizable ethylene sequences than the middle type chains. Mixing linear chains with branched chains enhanced the crystallizability of the branched chains, regardless of the type. In fact, the *t*/*g* ratios of the branched chains in the blend models are significantly higher than those of the respective pure branched chain models. It was found that the linear chains crystallized at a higher rate than the branched chains and thereby acted as nucleating sites for the crystallization of the branched chains. And it seems that both the linear and branched chains transversed through different ordered regions, thus forming the "tie chains". Nonetheless, the most interesting observation was that the blend that contained both types of branched chains exhibited an unexpectably high degree of order, comparable to those branched chains in the models containing linear chains. The finding seems to be attributed to the clustering of all the branches from both types of branched chains during the high-temperature annealing. In fact, the solid-state structure of such a blend contained essentially no "tie chains", and all branched chains adopted an adjacent reentry mode to form their own ordered regions. Finally, it should be pointed out that the above conclusions are specific to the LLDPE models we used.

1. Introduction

Linear-low-density polyethylene (LLDPE) is a class of polyethylene that it is made up of molecules containing a linear chain of ethylene repeating units and short branches that are attached to the linear chain at various positions. Chains in most commercial LLDPE contain about 10−20 branches per 1000 backbone carbons. And the length of the branches varies from 2 (ethyl branches) to 6 carbons (hexyl branches). The number of branches greatly affects the crystallization behavior, thereby solid-state properties, of the polymer. And it has been observed that locations of branches also play a similar role. It is well-known that LLDPEs synthesized using different catalysts yield rather different solid-state properties even though such LLDPEs have comparable average number of branches.[1] In particular, Ziegler−Natta (ZN) catalyst tends to incorporate most of the branches in the low molecular weight chains while the single-site (ss) catalyst tends to yield more homogeneous distribution of branches among chains with different molecular weights. It is generally believed that branches on a given chain, regardless of its molecular weight, distribute randomly along the chain. However, recent temperature rising elution fractionation (TREF) experiments suggest that this may not be the case.[2] Since no analytical technique is available to measure intrachain branch distribution, a systematic study of the effect of how intrachain branch distribution on the solid-state structure of LLDPE is still a formidable challenge. At present, molecular dynamics (MD) simulation seems to be the only technique available for exploring the intrachain branch distribution dependency of LLDPE structure. In fact, Zhang et al. recently demonstrated that MD simulation could be used to capture the effect of interchain branch distribution homogeneity (ZN- vs ss-LLDPE) on their solid-state structures using multiple chain models in their corresponding condensed states.[3] And their simulation results are in good agreement with the solid-state structures of comparable LLDPEs revealed by the solid-state ^{13}C NMR spectroscopy.[4] Therefore, in this study, we further the simulation strategy used by these authors to explore how the intrachain branch distribution of LLDPE affects their solid-state structure.

Table 1. LLDPE Models Used in the Present Work

model	types of chains	density at 463 K, g/cm^3	number of chains
1	end type	0.759	10
2	middle type	0.759	10
3	end and middle types	0.759	5 each type
4	end and linear types	0.759	5 each type
5	middle and linear types	0.759	5 each type

2. LLDPE Models and Simulation Details

As schematically depicted in Figure 1, two types of LLDPE model chains were used in the present work. One type contained branches that clustered near one chain end (end type) while the other clustered around the chain middle (middle type). Each type of chains contained 300 methylene units and 3 hexyl branches that were apart from each other by 10 methylene units. The branch that was closer to the chain end in the end type LLDPE was connected to the sixth backbone carbon atom. Linear model chains, also containing 300 methylene units, were also used to study how they affect the crystallization of the

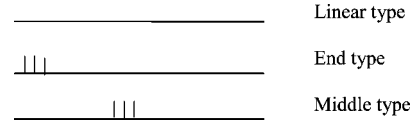

Figure 1. Chain architectures.

* To whom correspondence should be addressed.

10.1021/ma8011015 CCC: $40.75
Published on Web 09/12/2008

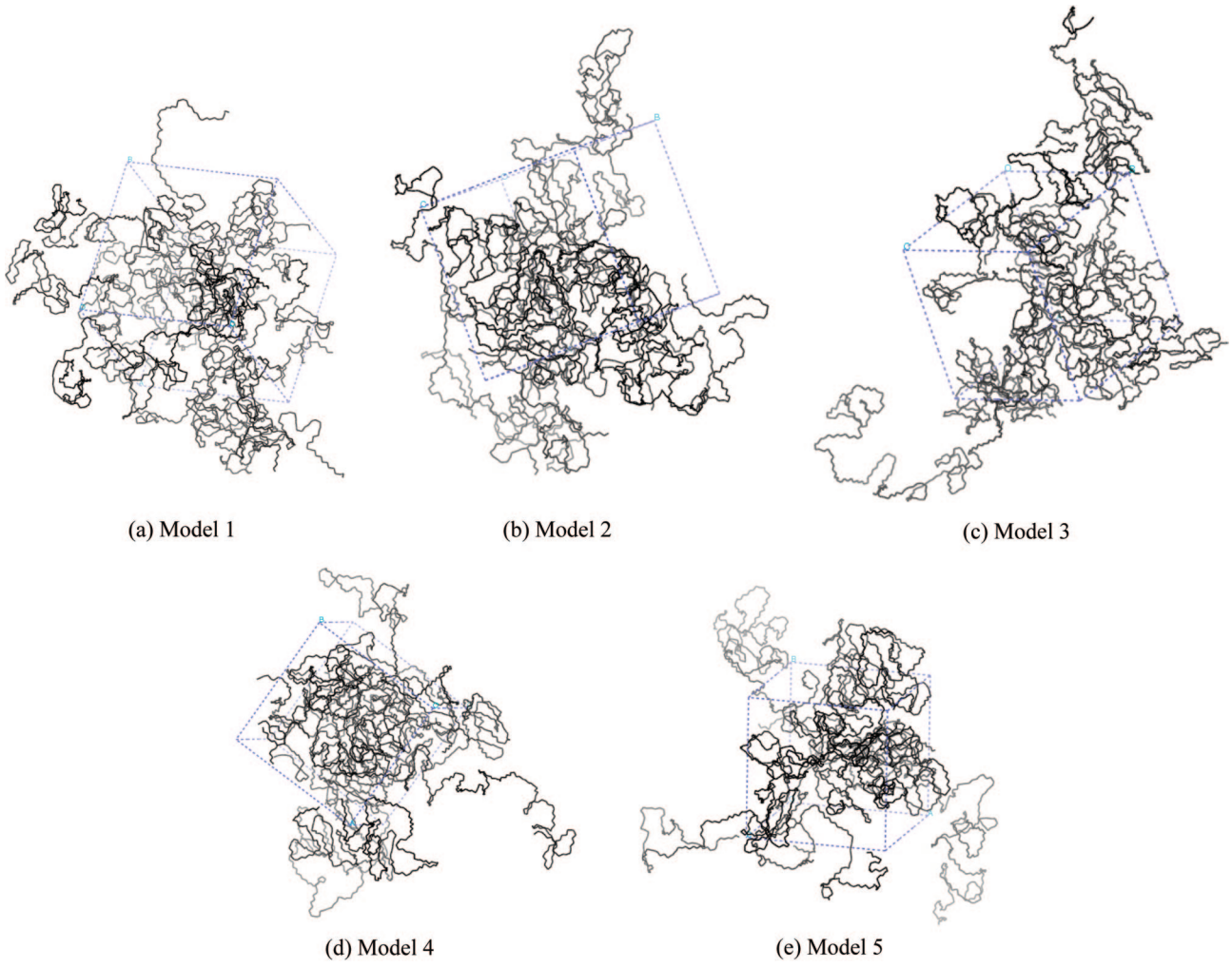

Figure 2. Initial structures of the five LLDPE models used in the canonical MD annealing at 463 K.

model LLDPE chains. All carbons in three types of chains were modeled with implicit hydrogen.

Five condensed state models containing different concentrations of the above model chains were constructed using the method of Theodorou and Suter along with the same melt density at 463 K.[5] It is worth noting that the melt density of polyethylene is independent of the average branch content.[6] The details of the models are summarized in Table 1. In particular, model 1 contained 10 end type chains while model 2 contained 10 middle type chains. The remaining three models were 50/50 mol/mol mixtures with different combinations of the linear chain and the other two types of LLDPE model chains. Such model mixtures also contained 10 chains. All initial structures were energy minimized before the high-temperature canonical (i.e., NVT) MD equilibration at 463 K. This equilibration step normally took about several nanoseconds. Once the systems were equilibrated, they were quenched to 373 K, a temperature slightly lower than the melting temperature of LLDPE, and tens of nanoseconds NVT MD annealing at the liquid density was carried out to mimic the early stage of the crystallization process.

All canonical MD simulations were performed using the Verlet algorithm along with the Nose thermostat for temperature control.[7] The integration time step was 1 fs. The force field used was Dreiding 2.21.[8] The choice of the force field was discussed elsewhere.[3] Nevertheless, Lennard-Jones parameters of united carbons developed by Rychaert and Bellemans were used.[9] All simulations were implemented on a Silicon Graphics workstation cluster with the use of commercial software Cerius[2] version 4.2.

3. Results and Discussion

3.1. Equilibration of the Liquid Structures. The initial structures of all five LLDPE models using the method of Theodorou and Suter[5] and the liquid structures after about 6 ns of NVT MD annealing at 463 K are presented in Figures 2 and 3, respectively. Apparently, structures after the high-temperature canonical MD annealing differ visibly. However, they all exhibit a fairly similar torsion angle distribution, calculated based upon the last 1 ns of the MD trajectories, that resembles very much to that of a polyethylene liquid (see discussion in ref 3). The results are not shown here as they are not of the main interest of the present work. To demonstrate that all model LLDPEs were properly equilibrated, we calculated the end-to-end vector orientation autocorrelation function (OACF) of all the models. Figure 4 shows that OACFs of all the systems decorrelate significantly at 463 K but stays more or less constant at 373 K, a temperature slightly lower than the melting temperature of LLDPE. Among the OACFs, the plateau value of model 2 reaches as low as about 0.2, while those of other models settle at about 0.35, indicating that chains with branches clustered around chain middles tend to exhibit more chain reorientation motion at 463 K and that linear chains and chains with branches clustered around chain ends would lessen such motion. Nevertheless, it is believed that all systems were subjected to adequate equilibration although the OACFs did not decorrelate to the limiting value of zero. This is because the calculated root-mean-square displacement (RMSDs) of the centers of mass of the chains over a period of 6 ns for each model is comparable

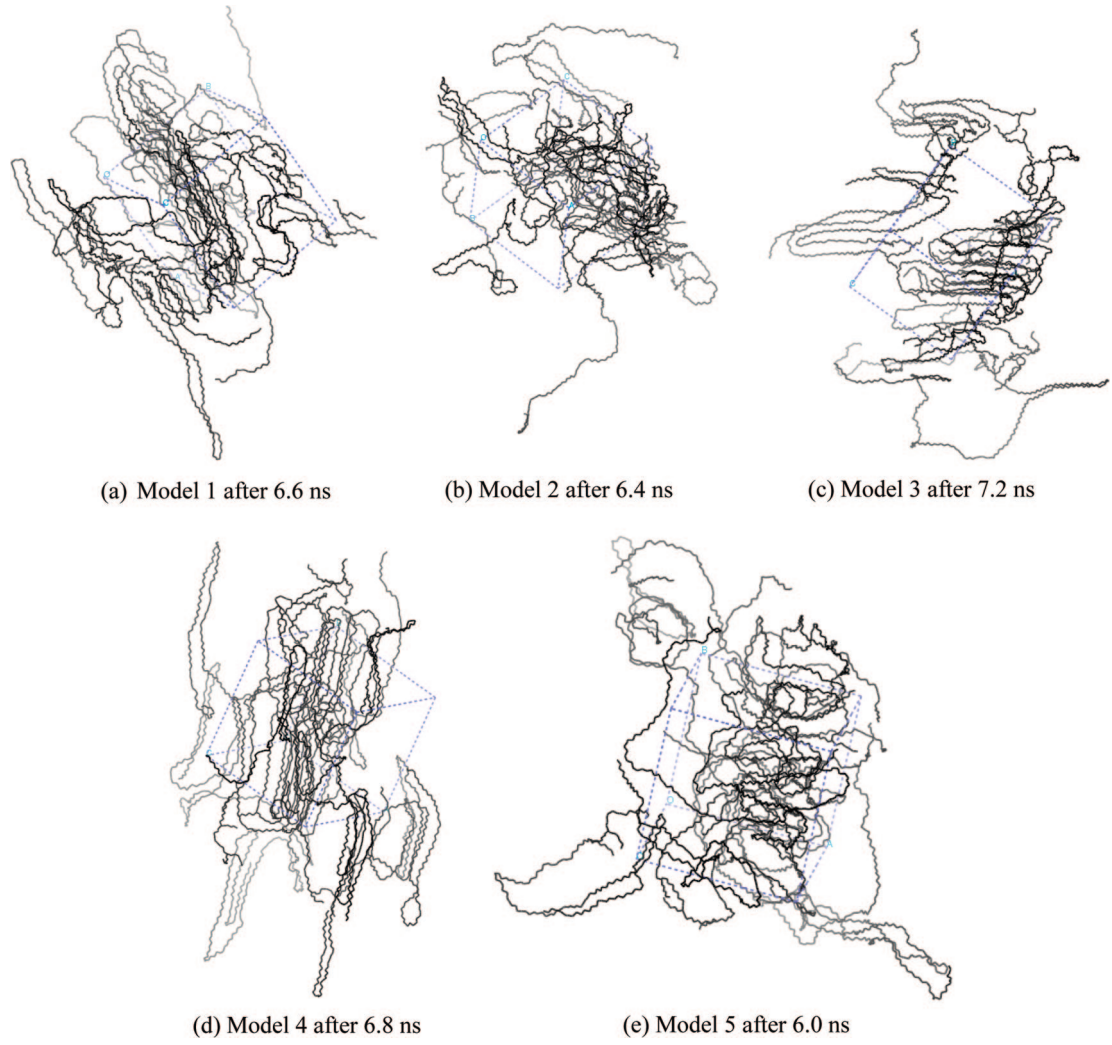

Figure 3. Liquid structures of the five LLDPE models after about 6 ns of MD annealing at 463 K.

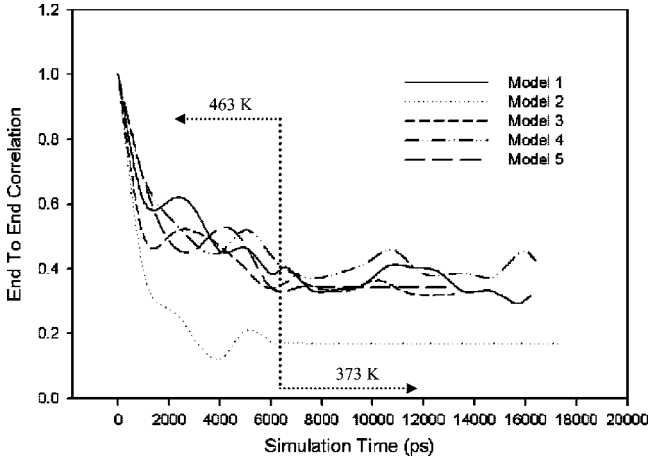

Figure 4. Computed end-to-end vector orientation autocorrelation functions of the five LLDPE models for both the high- and low-temperature canonical MD annealings.

to or greater than the corresponding average radii of gyration (see Table 2). The local order observed in the LLDPE models (low branch content) at 463 K simply shows that the molecular dynamics simulation strategy we used could reproduce the local order in polyethylene liquids experimentally observed by Pieper and Kilian.[10] Also, in our previous work in which an identical simulation strategy was used,[3] we have demonstrated that the computed structure factor of a liquid polyethylene model, which also contained a certain amount of apparent local order, agrees well with the experimental structure factor of a comparable polyethylene sample determined using X-ray diffraction at the Oak Ridge National Laboratory.

Table 2. Computed Root-Mean-Square Displacements (RMSD) of the Centers of Mass of All Chains and Radii of Gyration (R_g) of the Five Models Described in Table 1

model	RMSD (Å)	R_g (Å)
1	24.8	23.4
2	24.5	24.7
3	27.9	26.0
4	28.2	28.9
5	27.7	21.8

3.2. Solid-State Structure. Using the structures shown in Figure 3 as the initial structures, canonical MD annealing at 373 K were carried out for about 10 ns to simulate the early stage of the crystallization process at the liquid density. Figure 5 depicts the solid-state structures formed after such low temperature annealing. Except model 2, all other models exhibit visibly fairly ordered structures that resemble to the lamellar structure. This was why we carried out an additional 10 ns of low-temperature MD annealing for model 2. Torsion angle distributions of all the models except model 2 no longer exhibit a liquid like distribution. Here, since the model systems are small, thereby containing no lamellae, it is practically very difficult to determine which portions of a chain are in the ordered regions. This is because it is rather subjective to define ordered

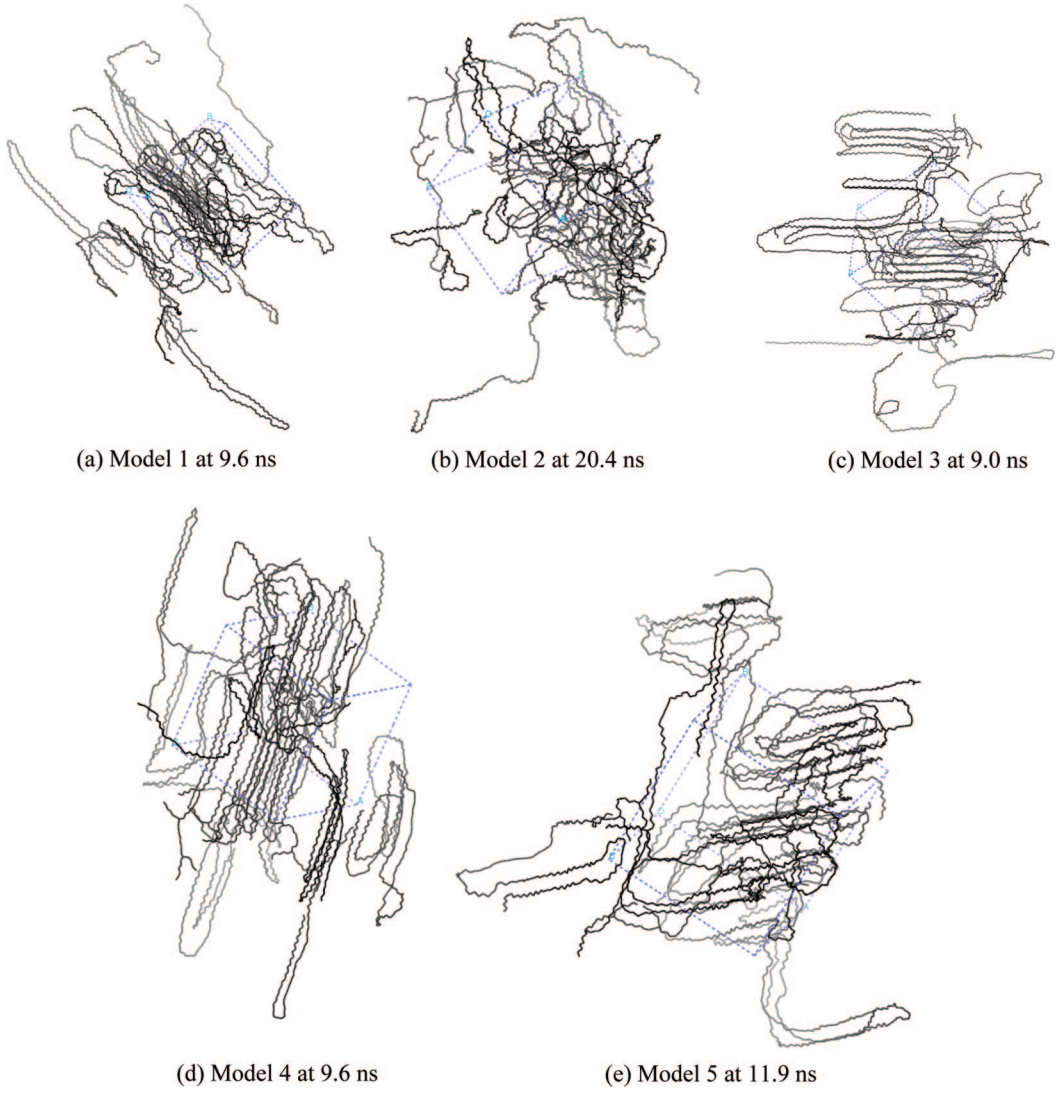

Figure 5. Solid-state structures of the five LLDPE models after about 10 ns canonical MD annealing at 373 K.

regions quantitatively for such small systems. Therefore, we use the overall *trans*/*gauche* (*t*/*g*) ratio to signify their degree of crystallinity. Obviously, overestimation of the degree of crystallinity is inevitable. As shown in Figure 6, the *t*/*g* ratios of the models increased as the low-temperature annealing proceeded and differ significantly toward the end of the annealing. In particular, model 1 shows a slightly higher *t*/*g* ratio comparing with model 2. It seems that chains in model 1 prefer to adopt an adjacent reentry mode to form the ordered region and leave all the chain ends (with the branches) residing in the region of less order. Nevertheless, a rather large fraction of chain segments are confined in the less ordered region. On the other hand, model 2 exhibits the lowest *t*/*g* ratio among all the models, suggesting that branches located around chain middles suppress the formation of lamellae.

Models 3−5 exhibit much higher of *t*/*g* ratios than those of the first two models. It was surprising to see that the *t*/*g* ratio of model 3 (*t*/*g* ratio is about 10, regardless the type of chains) is substantially higher than those of models 1 and 2 (*t*/*g* ratios are about 8 and 6, respectively) and is comparable to those of models 4 and 5 that contain linear chains. On examination of the individual chain conformation in model 3, almost all the chain segments are involved in the ordered regions except those near the branches. Another observation is that there seems no obvious difference between the conformations of the end type and middle type chains in such a system. As to model 4, almost all linear type chains were involved in the visibly more ordered regions while a relatively larger number of segments in the chains with branches resided in the less ordered region, especially those segments near the branches. Model 5 exhibits very similar structure to what was observed in model 4.

The observation that the branched chains in the blend models possess higher amounts of order (higher *t*/*g* ratios) than the two pure models indicates that blending help increase the crystallizability of branched chains, regardless of the type of branched chains (see Figure 6b). In models 4 and 5, it is probably attributed to the fact that the linear chains formed the ordered regions in a higher rate that they acted as nucleating sites for the branched chain to "crystallize". This is consistent with previous simulation results and experimental results of Mirabella.[3,11] Upon examination of the individual chain conformation, it seems that both linear and branched chains in models 4 and 5 did go through different ordered regions. And it is speculated that the reason why mixing of different types of branched chains could promote the formation of ordered regions is that during the high-temperature annealing, all branches from both types of branched chains were clustered together, thereby increasing the chances of the linear portion of the branched chains to crystallize. This is supported by the observation that different types of branched chains adopted the adjacent reentry mode to form their own ordered regions with little chains interpenetration.

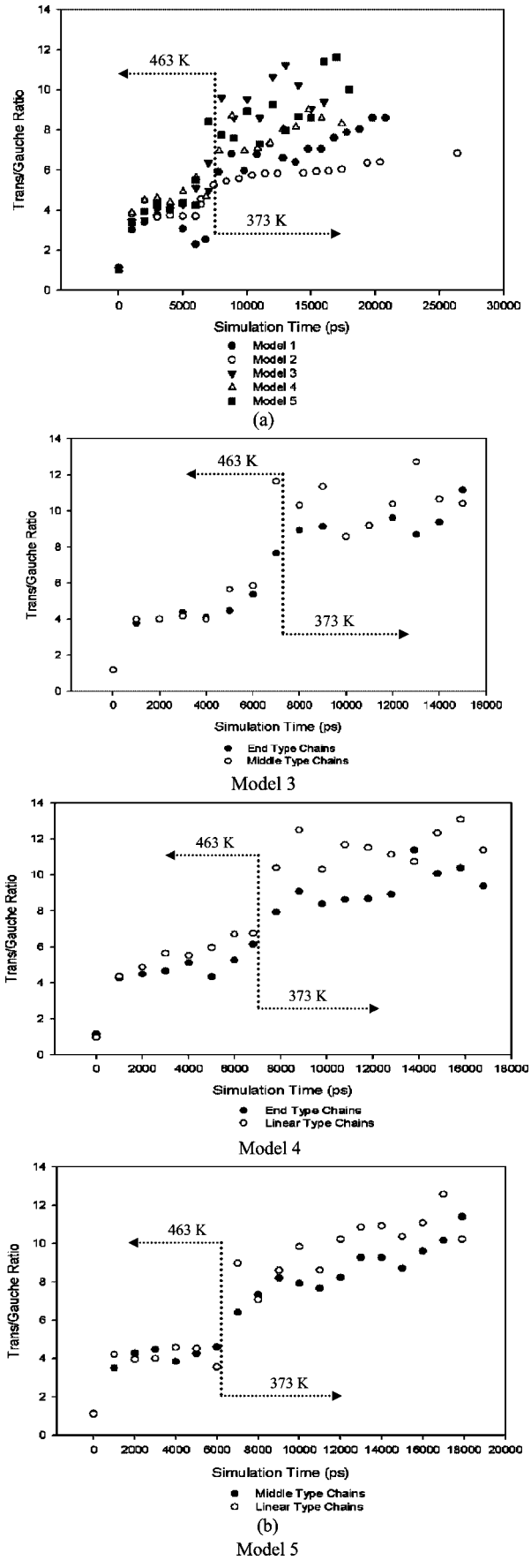

Figure 6. (a) Computed *trans*/*gauche* ratios of the five LLDPE models. (b) Computed *trans*/*gauche* ratios of chains with different molecular structures used in models 3−5.

Another noteworthy observation is that ordered regions (can be thought of as the lamellar stems) formed in all the five models consist of, on average, about 34 carbon atoms which are much longer than that of a comparable ss-LLDPE model previously reported (24 carbon atoms for chains with the same branch content as what was used in the present work but with the branches randomly distributed along the skeletal chains). This may be attributed to the fact that branches clustered in a small region of the chains make the crystallizable sequences of the chains longer than those found in the models with the same number of branches but distributed randomly along the skeletal chain.

Our previous simulation results revealed that the interchain branch homogeneity plays an important role in determining tie molecule concentration. In this work, we also examined the individual chain conformations of each model to infer the tie molecule concentration. It seems that chains in both models 4 and 5 tend to transverse through more than one ordered region, thereby leading to higher concentration of tie molecules. On the other hand, although model 3 shows a higher degree of order, the tie molecule concentration is rather low compared to those of models 4 and 5. This is because chains in model 3 tend to adopt the adjacent reentry mode when the order region was formed.

Finally, it should be pointed out that our conclusions are specific to the LLDPE models we used. In reality, difference in the molecular weight distribution and inhomogeneity in the intramolecular branch distribution of LLDPE would definitely lead to different solid-state structures. In principle, one could use larger multiple chain models to examine such effects. However, the required computational cost is so high that it is not feasible to do so at the time being.

4. Concluding Remarks

In this work, solid-state structures of LLDPEs with blocky branches clustered around chain ends and chain middles as well as their blends were studied using MD simulation. A total of five LLDPE models (two pure and three blend models) were used. All model structures were subjected to high-temperature canonical (NVT) MD annealing at 463 K before they were quenched to a temperature (373 K) that is slightly lower than the melting temperature of LLDPE. Our simulation results show that solid-state structures of LLDPEs are greatly affected by the intrachain branch locations and that blending branched chains with different intrachain branch distributions and with linear chains increases the degree of crystallinity, as quantified by the *t*/*g* ratio, for all the blend models as well as tie molecule concentration, except the model that contained different types of branched chains. Obviously, the conclusions are specific to the LLDPE models we used. Nevertheless, this work yielded molecular level insight into how intrachain branch distribution of blocky branches affects solid-state structure of LLDPEs that is difficult to obtain experimentally.

Acknowledgment. We thank the Natural Science Research Council of Canada for supporting this work financially. This research has been enabled by the use of WestGrid computing resources, which are funded in part by the Canada Foundation for Innovation, Alberta Innovation and Science, BC Advanced Education, and the participating research institutions. WestGrid equipment is provided by IBM, Hewlett-Packard, and SGI.

References and Notes

(1) Guichon, O.; Seguela, R.; David, L.; Vigier, G. *J. Polym. Sci., Part B: Polym. Phys.* **2003**, *41*, 327.
(2) Zhang, M.; Lynch, D. T.; Wanke, S. E. *Polymer* **2002**, *43*, 1497.
(3) Zhang, M.; Yuen, F.; Choi, P. *Macromolecules* **2006**, *39*, 8517.
(4) Wang, M.; Bernard, G. M.; Wasylishen, R. E.; Choi, P. *Macromolecules* **2007**, *40*, 6594.

(5) Theodorou, D. N.; Suter, U. V. *Macromolecules* **1985**, *18*, 1467.
(6) Rudin, A.; Chee, K. K.; Shaw, J. H. *J. Polym. Sci., Part C: Polym. Symp.* **1970**, *30*, 415.
(7) Nose, S. *J. Chem. Phys.* **1984**, *81*, 511.
(8) Mayo, S. L.; Olafson, B. D.; Goddard, W. A., III *J. Phys. Chem.* **1990**, *94*, 8897.
(9) Gychaert, J. P.; Bellemans, A. *Chem. Phys. Lett.* **1975**, *30*, 123.
(10) Kilian, H. G.; Pieper, T. *Adv. Polym. Sci.* **1993**, *108*, 49.
(11) Mirabella, F. M. *J. Polym. Sci., Part B: Polym. Phys.* **2001**, *39*, 2800.

MA8011015